Energy-Efficient for UAV-Assisted Vehicular Networks Under the Two-ways Street: Joint UAV Trajectory Optimization and Robust Power Control Approach

Zhixin Liu, Jianshuai Wei, Jiawei Su, Kit Yan Chan, Yazhou Yuan

***Abstract*—UAV-assisted Telematics mission offloading as an airborne base station is a promising solution, especially on two-way driving roads. This paper proposes a scheme to maximize energy efficiency in UAV-assisted Telematics and applies it to scenarios where both ground and air base stations are present on two-way streets. However, the stability of the transmission for the offloading task can be seriously affected by the uncertain channel state. To model channel uncertainty, we employ a first-order Markov process and take into account the vehicle's mobility. Real-time optimization of UAV flight trajectory can improve the quality of service for auxiliary vehicle communication. Additionally, energy consumption is a crucial concern for UAVs in the system. The Dinkelbach method is used to solve non-convex fractional programming optimization problems while maximizing energy efficiency. A power control and UAV trajectory planning algorithm for maximizing energy efficiency is proposed to determine the optimal solution. Numerical simulations are performed to evaluate the algorithm's performance. The results demonstrate its effectiveness, particularly when compared to other UAV and one-way lane scenarios.**

***Index Terms*—Internet of Vehicle (IoV), Computation Offloading, Robust Power Control, Edge Computing, UAV Communication,Trajectory Optimisation**

I. Introduction

A scenario similar to the one in literature [1] for maximising the energy efficiency of drone-assisted vehicular networks under two-way lanes was investigated [2], and in literature [3] the study The benefits about two-way lane communication are explored, vehicles travelling at high speed on a two-way highway [4], the ground base station is located on one side of the road, with the high speed of the vehicles travelling in the opposite direction [5], the vehicles travelling to the right will gradually drive out of the current communication cell, and can't communicate with the ground base station, at this time, the UAV can be used as an airborne base station in order to receive the communication signal from the vehicles. The UAV flies parallel to the road at a fixed altitude without any obstacles, and our proposed algorithm can determine in real time how to select the communication object for the vehicle in the current time slot to maximise the energy efficiency of the system. The contributions of this chapter can be summarised as follows: firstly, this chapter proposes a system model for planning UAV trajectories in a UAV-assisted two-way lane scenario, in order to improve the energy efficiency of the whole network system, we adopt the Dinkelbach method with a pricing mechanism so that the system can maximise the total throughput with minimum energy consumption, and in order to ensure the quality of service for the users of the ground vehicles, we establish a time-varying in the optimisation problem. probabilistic constraints under the vehicle movement model to describe the channel uncertainty as well as possible.

Zhixin Liu, Jianshuai Wei, Jiawei Su and Yazhou Yuan are with the School of Electrical Engineering, Yanshan University, Qinhuangdao 066004, China. Emails: lzxauto@ysu.edu.cn, jswe@stumail.ysu.edu.cn, Sjw@stumail.ysu.edu.cn, yzyuan@ysu.edu.cn.

Kit Yan Chan is with the School of Electrical Engineering, Computing and Mathematical Sciences, Curtin University, Perth, Australia. Email: k-it.chan@curtin.edu.au.

This work is supported partly by National Natural Science Foundation of China under Grant 62273298, 62273295.

A. Related Works

B. Contributions

In this paper, a scheme to maximize energy efficiency in vehicular networking by using UAV assistance for task offloading. The scheme is designed for vehicles dynamically traveling on two-way streets. Unlike existing studies that consider fixed base stations in one-way lanes, this paper investigates a network system that places great emphasis on UAV trajectory optimization in cooperation with power control. The scheme ensures the quality of vehicular communication through outage probability constraints. To summarize, this paper's primary contributions can be outlined as follows:

- An optimal vehicular communication scheme is proposed by integrating UAV-assisted vehicular communication with task offloading. This scheme efficiently finds the vehicle-selected offloading base station in Two-ways Street through UAV trajectory optimization.
- The first-order Markov process is used to handle the channel uncertainty caused by the high-speed movement of the vehicular network environment. Probabilistic constraints are employed to ensure vehicle QoS, and an integral transform approach is used to approximate non-convex probabilistic constraints in large-scale dynamic vehicular network environments.
- By optimizing the transmit power of the vehicle, the trajectory optimization of the UAV, and the allocation of time slots, and by proposing a scheme to transform the nonconvex problem using Dinkelbach's algorithm, the energy efficiency of the system is successfully maximized.

The rest of this paper is organized as follows: the model energy efficiency in vehicular networking by using UAV assistance for task offloading is presented in Section II. In Section III, the objective function and the non-convex constraints are formulated, and the problem solutions are proposed. In Section IV, the performance evaluations are presented. Finally, we conclusion the paper in Section V.

II. System model

In this chapter, an integrated heaven and earth network is considered, in which vehicles are travelling on a bi-directional highway, and UAVs take off from the vicinity of the base station and cache the resources provided by the base station for downloading by the vehicles on the road, since it is a bi-directional lane, the base station is located at the origin of the coordinates at a height of h_0, and the D_R represents the radius length of the coverage of the roadside cell, and in order to consider a more realistic road scenario, we model the vehicle motion as a constant velocity motion model [6]. We specify rightward as the positive direction, and define the lane index $L = 1$ as the vehicle travelling to the right and $L = -1$ as travelling to the left. Due to the fixed location of the base station, with the passage of time, there is inevitably a direction of the vehicle will be far away from the base station, which will inevitably affect its access to information through the base station, at this time, the UAV flew towards the right side of the base station, which in turn helps the vehicle away from the base station to obtain the required information. In order to decide whether the vehicle on the road needs to obtain information from the drone or the base station, we based on the channel state information predicted by the first-order Markov process from the vehicle to the base station and the channel state information obtained by the vehicle and the aerial base station drone line-of-sight link to the vehicle and the two data in the centre of the communication of the signal-to-noise ratio, respectively, the vehicle will choose the party with the larger signal-to-noise ratio to request resources, $x_m[t] = 1$ for the vehicle to select the UAV for communication, and vice versa for the vehicle to select the base station for communication.

In the time slot t, the horizontal coordinates of the drone are $q_U[t] = \{x_u[t], y_u[t]\}$. The UAV is flying unobstructed at a height of H from the road surface with a maximum speed of V_{max} and the initial horizontal position of the vehicle M is $q_M[0] = \{x_0, y_0\}$. Assuming that the vehicle is travelling at speed ν_m in a uniform straight line, based on the previously defined lane index it can be derived that the vehicle M at the tth moment of the water The horizontal position changes to $x_m[t] = x_0 + l\nu_m t$, and the horizontal position of vehicle M $q_M = \{x_m[n], y_0\}$. Based on the position information we can get the distance information at the tth moment The distance between vehicle M and the roadside unit at t time slot is $d_{m,R}[t] = \|q_M[t] - q_R\| = \sqrt{x_m[t]^2 + {y_0}^2 + H^2}$,The distance of vehicle M from the UAV at t time slot is $d_{m,U}[t] = \|q_M[t] - q_U[t]\| = \sqrt{(x_m[t] - x_u[t])^2 + (y_m[t] - y_u[t])^2 + H^2}$. The system model is shown in Fig. 1. Furthermore, some notations used in this paper are given in Table I.

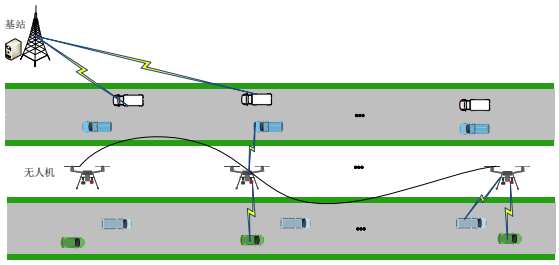

Fig. 1:

TABLE I: Notations

$\Pr\{\cdot\}$	Probability function.
$\mathrm{q}[t]$	UAVs position at slot t.
$\mathbb{R}^k$	Set of k-dimensional real vectors.
$\mathbf{q}$	Index set of UAV trajectory optimization $\mathbf{q}$=$[q_1, \cdots, q_i, \cdots, q_M]$.
$\mathbf{p}$	Index set of vehicle power $\mathbf{p}$=$[p_1, \cdots, p_i, \cdots, p_M]$.
$\mathcal{T}$	Index set of time slot $\mathcal{T}$=$\{1, 2, \cdots, T\}$.
$\mathcal{M}$	Index set of all active vehicles $\mathcal{M}$=$\{1, 2, \cdots, M\}$.
$\mathrm{E}\{\cdot\}$	Expected value of a random variable.

A. Channel and Energy Consumption Models of V2R Communication

Due to the rapidity of vehicle movement, for the V2I communication between the vehicle and the roadside unit, a first-order Markov process similar to the one in the previous chapter is constructed, where the channel state information at the tth moment is predicted from the state prediction of the previous moment. i.e.

$$h_m = \widetilde{h}_m^2 + \hat{h}_m^2, \tag{1}$$

Here $\widetilde{h}_m$ is an observation and $\hat{h}_m$ is an exponential distribution obeying the parameter $a = \frac{1}{{L_{i,j}^k}^2(1-{\zeta_{i,j}^k}^2)}$. The signal-to-noise ratio (SNR) of the mth vehicle received by the ground base station at the tth time slot can be expressed as:

$$\gamma_{m,R}[t] = \frac{p_m[t] h_{m,R}[t]}{\sigma^2} \tag{2}$$

According to Shannon's capacity theorem, the transmission rate from the vehicle to the terrestrial base station can be expressed as:

$$R_{m,R}[t] = \log_2(1 + \gamma_{m,R}[t]) \tag{3}$$

The amount of data transmitted by the vehicle to the terrestrial base station can be expressed as.

$$L_{m,R} = B_0 \sum_{m=1}^{M} \sum_{t=1}^{T} x_m[t] R_{m,R}[t], \tag{4}$$

Where B_0 denotes the bandwidth and $x_m[t] = 1$ indicates that the vehicle has chosen to transmit data to the terrestrial base station at the current moment and $x_m[t] = 0$ vice versa.

$$E_{m,R} = \sum_{m=1}^{M} \sum_{t=1}^{T} x_m[t] p_m[t] \tag{5}$$

B. Channel and Energy Consumption Models of V2U Communication

For the communication between the vehicle and the UAV without obstacle occlusion in the middle, which is a line-of-sight link, an airborne RF link model is constructed, and the channel gain from the m vehicle to the UAV at tth time slot is

$$h_{m,U}[t] = \frac{\varsigma_0}{d_{m,U}[t]^2} \tag{6}$$

Here ς_0 is the power gain per unit distance of 1 metre, with the above information, the transmission rate from UAV to vehicle is

$$R_{m,U}[t] = \log_2(1 + \gamma_{m,U}[t]), \tag{7}$$

$$\gamma_{m,U}[t] = \frac{p_m[t] h_{m,U}[t]}{\sigma^2}, \tag{8}$$

where denotes the signal-to-noise ratio of the vehicle-to-UAV communication, and the amount of data transmitted by the vehicle to the UAV airborne base station can be expressed as

$$L_{m,U} = B_0 \sum_{m=1}^{M} \sum_{t=1}^{T} x_m R_{m,U}[t], \tag{9}$$

Where B_0 denotes the bandwidth, the transmission energy consumption of a vehicle communicating to an airborne base station UAV is calculated as follows.

$$E_{m,U} = \sum_{m=1}^{M} \sum_{t=1}^{T} y_m[t] p_m[t] \tag{10}$$

Since there is a good line-of-sight link between the UAV and the roadside unit, we believe that the data sent from the vehicle to the UAV can be efficiently transmitted to the ground base station and processed by the edge server attached to the roadside unit.

C. Vehicle Computing Task Offloading and Energy Model

The edge server attached to the roadside unit can perform data computational processing for the received vehicle data, so the computational offloading process requires computational resources to perform the subtasks split by the collaborative computational model. The entire computational task for the mth vehicle is denoted as A_m, and at some time slot when it splits the task to the roadside unit it is denoted as $A_{R,m} = z_m A_m$ Defining f_R as the acceleration frequency of the CPU of the edge server of the roadside unit, the computation time can be expressed as:

$$t_m^{mec} = \frac{A_{R,m}}{f_R} \tag{11}$$

The time taken by the vehicle to complete the task upload and computation is the sum of the fixation time when the roadside unit sends data to the edge server and the computation time, which should be less than the traveling time of the vehicle within the unit's coverage area in order to ensure the smooth transmission of the task and its computation.

The computational energy consumption of the edge server after the mth sub-task needs to be uploaded is:

$$E_m^{mec} = \aleph A_{R,m} {f_R}^2 \tag{12}$$

where $\aleph > 0$ is the effective switching capacitance of the CPU, depending on the chip architecture.

D. Problem Formulation

In this section, we formulate the energy efficiency maximisation problem for UAV-assisted two-way lane vehicles. We aim to maximise the total energy efficiency of the system by jointly optimising the transmit power of the vehicles on the two-way lanes as well as the trajectory of the UAV. First, the energy efficiency of this network communication system is defined as

$$EE(\mathbf{P}, \mathbf{Q}) = \frac{L_m(\mathbf{P}, \mathbf{Q})}{E_m(\mathbf{P})} \tag{13}$$

Where $L_m = L_{m,R} + L_{m,U}$ is the total amount of data sent by the vehicle to the ground base station and the aerial base station, and $E_{m,R}$ and $E_{m,U}$ are the energy consumptions of the vehicle and the ground base station aerial base station respectively. Since there will be energy consumption during the UAV flight, we will pay more attention to the energy consumption when the vehicle communicates with the UAV and consider the energy trade-off between the air base station communication and the ground base station communication, so the total power consumption of the system is expressed as $E_m = (1-\theta)L_{m,R} + \theta L_{m,U}$, where $0 \leq \theta \leq 1$ is a weighting factor for the energy cost of the vehicle when communicating with the UAV. When θ is large it means that we are more concerned about the energy cost of the UAV. The final system energy efficiency maximisation problem is formulated as follows:

$$\mathbf{P}: \quad \max_{\mathbf{P},\mathbf{Q},\mathbf{X}} EE(\mathbf{P}, \mathbf{Q}, \mathbf{X}) \tag{14}$$

$$\text{s.t. } \Pr\{x_m[t]\gamma_{m,R}[t] + y_m[t]\gamma_{m,U}[t] \geq \gamma_{th}\} \geq 1 - \varepsilon_3, \forall m, t \tag{14-1}$$

$$0 \leq p_m[t] \leq p_{max}, \forall m \tag{14-2}$$

$$x_m[t] + y_m[t] = 1, \forall m \tag{14-3}$$

$$\frac{D_R}{\nu_m} \geq t_m^{mec} + t_{wired} \tag{14-4}$$

$$q_U^{n+1} - q_U^n \leq tV_{max}, \forall m \tag{14-5}$$

The (14-1) in the above equation represents the interruption probability constraint to ensure the quality of service by guaranteeing vehicle communication, the (14-2) gives the constraint on the maximum and minimum transmit power of the vehicle, the (14-3) represents the fact that the task of each vehicle at each moment in time can only be offloaded to either the UAV or the terrestrial base station, γ_{th} is the threshold of the signal-to-noise ratio as a fixed value, (14-4) represents the need to dispatch the vehicle before it leaves the roadside cell coverage area. before the server has to complete the computation of the completion data, and the allocation of time slot resources can be carried out by this constraint, where t_{wired} is the time when the roadside unit sends data to the edge server for a fixed time. The flight trajectory of the UAV is constrained by (14-5), i.e., the actual distance flown by the UAV per second must be less than or equal to the maximum flyable distance of the UAV.

III. SOLVING THE EE MAXIMIZATION PROBLEM

In this section, the energy efficiency maximisation problem from the previous section is broken down into two sub-problems to be solved. For the fractional programming which is difficult to solve, it can be solved by using Dinkelbach's method to transform it into an easy-to-solve reduced-form programming. First fix the vehicle's launch power and then solve for the UAV's flight trajectory, then fix the UAV's flight trajectory and then solve for the vehicle's launch power, and so on in alternating iterations of optimisation until the algorithm converges. Noting that question (14) in the previous section is a non-convex problem, we propose a joint power allocation and UAV trajectory planning scheme to deal with this problem efficiently by decoupling the problem (14) into three subproblems [7].

A. Probabilistic Constrained Approximation and Optimal Power Control Problems

In the previous section of the equation (14-1) we found that the vehicle's power power in the probabilistic constraints in the existence of more complex coupling relationship, is difficult to solve directly, is difficult to solve.For this situation, we will use the integral transformation to transform the complex probability constraint problem into a simpler form.

Theorem: For (14-1), the interruption probability constraints of vehicle users

$$\Pr\left\{x_m\left[t\right]\gamma_{m,R}\left[t\right]+y_m\left[t\right]\gamma_{m,U}\left[t\right]\geq\gamma_{th}\right\}\geq1-\varepsilon_3$$

Equivalent:

$$\begin{aligned}p_m\left[t\right]x_m\left[t\right]\ln\left(1-a\varepsilon_3\right)+\left(\gamma_{th}-y_m\left[t\right]\gamma_{m,U}\right)\left[t\right]a\sigma^2\\\leq ap_m\left[t\right]x_m\left[t\right]\hat{h}_m\left[t\right]\end{aligned}\tag{15}$$

proof:

$$\frac{x_m\left[t\right]p_m\left[t\right]h_{m,R}\left[t\right]}{\sigma^2}\geq\gamma_{th}-y_m\left[t\right]\gamma_{m,U}\left[t\right]\tag{16}$$

$$\Leftrightarrow p_m\left[t\right]\widetilde{h}_m\left[t\right]\geq\frac{\left(\gamma_{th}-y_m\left[t\right]\gamma_{m,U}\left[t\right]\right)\sigma^2}{x_m\left[t\right]}-p_m\left[t\right]\hat{h}_m\left[t\right]$$

Therefore the vehicle user's interruption probability constraint makes a reformulation as follows:

$$Pr\left\{x_m\left[t\right]\gamma_{m,R}\left[t\right]+y_m\left[t\right]\gamma_{m,U}\left[t\right]\geq\gamma_{th}\right\}\geq1-\varepsilon_3\tag{17}$$

$$\Leftrightarrow\Pr\left\{\widetilde{h}_m\left[t\right]\geq\frac{\left(\gamma_{th}-y_m\left[t\right]\gamma_{m,U}\left[t\right]\right)\sigma^2}{p_m\left[t\right]x_m\left[t\right]}-\hat{h}_m\left[t\right]\right\}\geq1-\varepsilon_3$$

Since the probability density function of the random variable $\widetilde{h}$ is $f_x=e^{-ax}$, it can be obtained by integral transformation:

$$\begin{aligned}&\int_0^{\frac{\left(\gamma_{th}-y_m\left[t\right]\gamma_{m,U}\right)\sigma^2}{p_m\left[t\right]x_m\left[t\right]}-\hat{h}_m\left[t\right]}e^{-ax}dx\leq\varepsilon_3\\&\Leftrightarrow p_m\left[t\right]x_m\left[t\right]\ln\left(1-a\varepsilon_3\right)+\left(\gamma_{th}-y_m\left[t\right]\gamma_{m,U}\left[t\right]\right)a\sigma^2\\&\quad\leq ap_m\left[t\right]x_m\left[t\right]\hat{h}_m\left[t\right]\end{aligned}\tag{18}$$

For ease of expression, we define $\gamma_{m,U}\left[t\right]=p_m\left[t\right]\eta_{m,U}\left[t\right]$the $\eta_{m,U}\left[t\right]=h_{m,U}\left[t\right]/\sigma^2$further $\kappa_m\left[t\right]=x_m\left[t\right]\ln\left(1-a\varepsilon_3\right)-y_m\left[t\right]\eta_{m,U}\left[t\right]a\sigma^2-ax_m\left[t\right]\hat{h}_m\left[t\right]$ Rewrite the equation (18) as.

$$p_m\left[t\right]\kappa_m\left[t\right]+a\sigma^2\gamma_{th}\leq0\tag{19}$$

The process of solving for the vehicle's transmit power requires each time slot to perform power rate allocation with UAV trajectory planning and multiple iterations. The subproblem on vehicle launch power $p_m\left[t\right]$ is described as follows:

$$\max_{\mathbf{P}}=\frac{L_m\left(\mathbf{P}\right)}{\left(1-\theta\right)E_{m,R}\left(\mathbf{P}\right)+\theta E_{m,R}\left(\mathbf{P}\right)}\tag{20}$$

$$\text{s.t. }(19),(14\text{-}4)\tag{20-1}$$

Notice that the problem (20) is a fractional planning problem, and in order to transform it into a subtractive planning problem, it is proposed to solve it using the Dinkelbach method.

$$\begin{aligned}F(\chi)=&\max_{\mathbf{P}}\sum_{t=1}^{T}\sum_{m=1}^{M}B_0x_m^{\{l\}}\left[t\right]\log_2\left(1+p_m\left[t\right]\eta_{m,R}^{\{l\}}\left[t\right]\right)\\&+\sum_{t=1}^{T}\sum_{m=1}^{M}B_0x_m^{\{l\}}\left[t\right]\log_2\left(1+p_m\left[t\right]\eta_{m,U}^{\{l\}}\left[t\right]\right)\\&-\chi\sum_{t=1}^{T}\sum_{m=1}^{M}\left(1-\theta\right)x_m^{\{l\}}\left[t\right]p_m\left[t\right]+\theta y_m^{\{l\}}\left[t\right]p_m\left[t\right]\\&\text{s.t. }(18),(14\text{-}4)\end{aligned}\tag{21}\tag{21-1}$$

$\eta_{m,R}^{\{l\}}\left[t\right]=h_{m,R}\left[t\right]/\sigma^2$ in the above equation. $\eta_{m,U}^{\{l\}}\left[t\right]=h_{m,U}\left[t\right]/\sigma^2$. Considered constant at every l iteration, for the convex problem (21). we can construct the Lagrangian function and apply the Lagrangian dyadic method to solve it:

$$\begin{aligned}&L\left(\mathbf{p},\lambda\right)\\&=\sum_{t=1}^{T}\sum_{m=1}^{M}B_0x_m^{\{l\}}\left[t\right]\log_2\left(1+p_m\left[t\right]\eta_{m,R}^{\{l\}}\left[t\right]\right)\\&+\sum_{t=1}^{T}\sum_{m=1}^{M}B_0y_m^{\{l\}}\left[t\right]\log_2\left(1+p_m\left[t\right]\eta_{m,U}^{\{l\}}\left[t\right]\right)\\&-\chi\sum_{t=1}^{T}\sum_{m=1}^{M}\left(1-\theta\right)x_m^{\{l\}}\left[t\right]p_m\left[t\right]+\theta y_m^{\{l\}}\left[t\right]p_m\left[t\right]\\&-\sum_{t=1}^{T}\sum_{m=1}^{M}\lambda_{m,t}\left(p_m\left[t\right]\kappa_m\left[t\right]+a\sigma^2\gamma_{th}\right)\end{aligned}\tag{22}$$

Where the Lagrange multiplier $\lambda_{m,t}\geq0$, the Lagrange pairwise function of (22) is expressed as:

$$D(\lambda)=\max_{0\leq P_m[t]\leq P_{\max}}L\left(\mathbf{p_m},\lambda\right)\tag{23}$$

where the dyadic problem of (23) is:

$$\min_{\lambda_{m,t}\geq0}D\left(\mathbf{p_m},\lambda\right)\tag{24}$$

The problem (24) is a convex problem and satisfies the Karush-Kuhn-Tucker (KKT) condition, which can be made to have a first-order derivative equal to zero in an analogous solution process using the KKT condition:

$$\begin{aligned}&\frac{B_0x_m^{\{l\}}[t]\eta_{m,R}^{\{l\}}[t]}{\ln2\left(1+p_m[t]\eta_{m,R}^{\{l\}}[t]\right)}+\frac{B_0y_m^{\{l\}}[t]\eta_{m,U}^{\{l\}}[t]}{\ln2\left(1+p_m[t]\eta_{m,U}^{\{l\}}[t]\right)}+\chi\left(\theta-x_m^{\{l\}}\left[t\right]\right)\\&-\sum_{t=1}^{T}\lambda_{m,t}\left(-y_m[t]\eta_{m,U}[t]a\sigma^2+x_m[t]\hat{h}_m[t]-\frac{x_m[t]a\varepsilon_3}{1-a\varepsilon_3}\right)=0,\end{aligned}\tag{25}$$

From the above equation

$$p_m\left[t\right]=\frac{x_m^{\{l\}}[t]}{\eta_{m,R}^{\{l\}}[t]}+\frac{y_m^{\{l\}}[t]}{\eta_{m,U}^{\{l\}}[t]} -\frac{B_0}{\ln 2\lambda_{m,t}\left[y_m^{\{l\}}[t]\eta_{m,U}^{\{l\}}[t]a\sigma^2+x_m^{\{l\}}\left(\hat{h}_m[t]-\frac{a\varepsilon_3}{1-a\varepsilon_3}\right)\right]} \tag{26}$$

For simplicity we make the $c_m\left[t\right]=y_m^{\{l\}}\left[t\right]\eta_{m,U}^{\{l\}}\left[t\right]a\sigma^2+x_m^{\{l\}}\left(\hat{h}_m[t]-\frac{a\varepsilon_3}{1-a\varepsilon_3}\right)$ According to (25), the power allocation is iteratively updated by

$$p_m[t]^*=\left[\frac{x_m^{\{l\}}\left[t\right]}{\eta_{m,R}^{\{l\}}\left[t\right]}+\frac{y_m^{\{l\}}\left[t\right]}{\eta_{m,U}^{\{l\}}\left[t\right]}-\frac{B_0}{\ln 2\lambda_{m,t}c_m\left[t\right]}\right]_0^{p_{max}} \tag{27}$$

We can update the Lagrange multiplier λ_m using the subgradient method as follows:

$$\lambda_m^{(i+1)}=\left[\lambda_m^{(t)}+\Delta_m^{(t)}G_{\lambda_m}\right]^+ \tag{28}$$

where G_{λ_m} represents the step size of the Lagrange multiplier and $G_{\lambda_m}\geq 0$. The variable i is the iteration index and the positive part of the variable x is defined as $[x]^+=\max\left[0,x\right]$. The Lagrange multipliers are updated by the subgradient method as follows

$$G_{\lambda_m}=p_m\left[t\right]\kappa_m\left[t\right]+a\sigma^2\gamma_{th} \tag{29}$$

B. UAV trajectory Optimization Design

The optimisation problem for the UAV trajectory can be solved as follows when the vehicle power allocation is obtained through the previous section: When the vehicle transmit power $\left\{P_m{}^{\{l\}}\right\}$ and the time slot allocation for each iteration are given, the optimisation with respect to the UAV trajectory is described as follows:

$$\max_{\mathbf{Q}}=\frac{L_{m,R}+L_{m,U}\left(\mathbf{Q}\right)}{(1-\theta)E_{\mathrm{t}}{}^{R,\{l\}}+\theta E_{\mathrm{t}}{}^{U,\{l\}}} \tag{30}$$
$$\text{s.t. (14-2)} \tag{30-1}$$

the

$$L_{m,U}\left(\mathbf{Q}\right)=\log_2\left(1+\frac{\varphi_{m,U}^{\{l\}}\left[t\right]}{\left\|q_M\left[t\right]-q_U\left[t\right]\right\|+H^2}\right) \tag{31}$$

Here $\varphi_{m,U}^{\{l\}}\left[t\right]=\frac{p_m^{\{l\}}[t]\varsigma_0}{\sigma^2}$. We note that the numerator part of the objective function of problem (30) is non-concave, and propose to approximate the objective function by a continuous convex approximation method. In $q^{\{l\}}\left[t\right]$ the local point of the first order Taylor expansion of the logarithmic form of the numerator part of Eq. (30) is performed as follows:

$$\log_2\left(1+\frac{\varphi_{m,U}^{\{l\}}\left[t\right]}{\left\|q_M\left[t\right]-q_U\left[t\right]\right\|+H^2}\right) \tag{32}$$
$$\geq\left(\omega_m^{\{l\}}\left[t\right]\left\|q_M\left[t\right]-q_U\left[t\right]\right\|^2-\left\|q_M\left[t\right]-q_U^{\{l\}}\left[t\right]\right\|^2+\rho_m^{\{l\}}\left[t\right]\right)$$
$$\triangleq R_{m,U}^{\{l\}}(\mathbf{q}[t])$$

and,

$$\omega_m^{\{l\}}\left[t\right]=\frac{-\varphi_{m,U}^{\{l\}}\left[t\right]}{\ln 2\left(\left\|q_M\left[t\right]-q_U^{\{l\}}\left[t\right]\right\|^2+H^2\right)}\cdot \frac{1}{\left\|q_M\left[t\right]-q_U^{\{l\}}\left[t\right]\right\|^2+H^2+\varphi_{m,U}^{\{l\}}\left[t\right]} \tag{33}$$

and,

$$\rho_m^{\{l\}}\left[t\right]=\log_2\left(1+\frac{\varphi_{m,U}^{\{l\}}\left[t\right]}{\left\|q_M\left[t\right]-q_U^{\{l\}}\left[t\right]\right\|+H^2}\right) \tag{34}$$

The problem (30) is further transformed into:

$$\max_{\mathbf{Q}}=\frac{L_{m,R}+\sum_{t=1}^{T}\sum_{m=1}^{M}B_0y_m^{\{l\}}\left[t\right]R_{m,U}^{\{l\}}(\mathbf{q}[t])}{(1-\theta)E_{\mathrm{t}}{}^{R,\{l\}}+\theta E_{\mathrm{t}}{}^{U,\{l\}}} \tag{35}$$
$$\text{s.t. (14-2)} \tag{35-1}$$

At this point, the non-convex part of the problem (30) is transformed into a convex solvable form that can be solved using the convex optimisation toolbox CVX.

C. Subslot Resource Allocation Problems

From the inequality (14-4) with $A_{R,m}=z_mA_m$, we learn that the allocation of time slots is constrained by the server's computation time, and thus can be easily obtained:

$$z_m=\sum_{t=1}^{T}x_m\left[t\right],\qquad\forall m\in\mathcal{M} \tag{36}$$

That is, all the time slots for the vehicle to communicate to the terrestrial base station add up to less than the vehicle is within the coverage area of the base station. When the power and trajectory are given, the subproblem on allocating time slots is as follows:

$$\max_{\mathbf{X},\mathbf{Y}}=\frac{L_{m,R}\left(\mathbf{X}\right)+L_{m,U}\left(\mathbf{Y}\right)}{(1-\theta)E_{\mathrm{t}}{}^{R,\{l\}}\left(\mathbf{X}\right)+\theta E_{\mathrm{t}}{}^{U,\{l\}}\left(\mathbf{Y}\right)} \tag{37}$$
$$\text{s.t. (14-3), (14-4)} \tag{37-1}$$

This is a fractional programming problem, and we can use a Dinkelbach method similar to that used for problem (20) to transform the original problem into an easily solvable reduced-form programming, i.e., equation (37) is equivalent to a linear programming problem that can be solved iteratively using the Convex Optimisation Toolbox (CVX).

D. Overall Algorithm Design

The original problem (14) is divided into three subproblems which have been solved separately in the above subsections. They are then solved alternatively using an alternating iteration method, which is shown in the following in Algorithm 1.

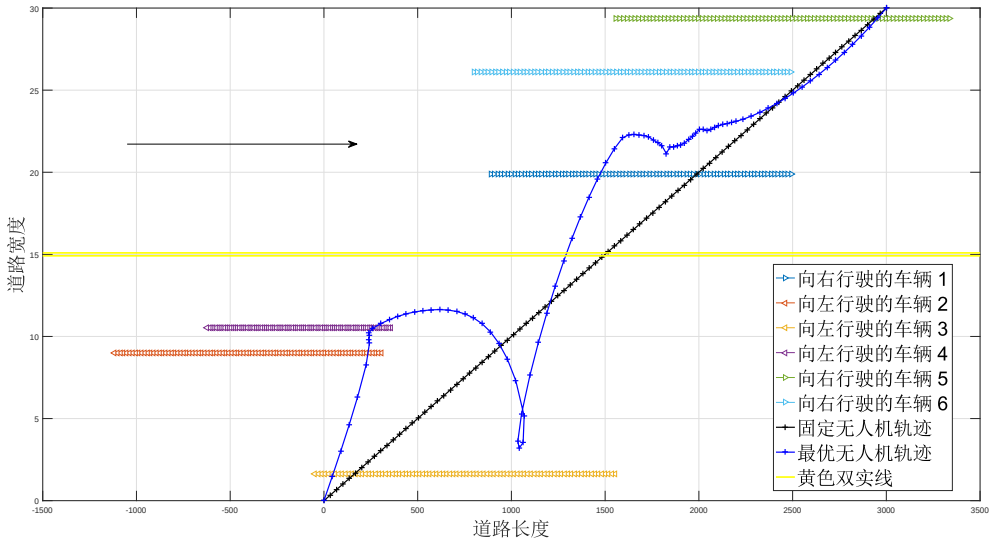

Fig. 2: Dual-arm robotic system.

Algorithm 1 Robust Power Control Task Offloading Scheduling Algorithm

1: **Input:** Set the maximum number of iterations $\mathcal{T}_{max}$, and the iterative index $t = 0$.
2: **repeat**
3: Initialize the feasible points λ, μ and $\mathbf{f}$.
4: Solve problem $\mathbf{P1}$, and determine the current optimal solution $\widetilde{p}^{(t+1)}$.
5: Initialize the feasible points ξ, φ and $\mathbf{p}$.
6: Solve the problem $\mathbf{P2}$, and determine the current optimal solution $\widetilde{f}^{(t+1)}$.
7: **until** algorithm converges synchronously to the optimal result or $t \geq \mathcal{T}_{max}$
8: **Output:** $\mathbf{f}, \mathbf{p}$.

TABLE II: System parameters

Parameter	Value
Radio Range (R_a)	300 m
Carrier frequency (f_c)	5.9 GHz
CSI feedback period of vehicle (T)	1 ms
Average speed of vehicle	30 m/s
Mean of background noise (σ^2)	-30 dBm
Maximum transmitter power ($p_{i,max}$)	0.05 W
threshold parameter	10^{-6}
UAV ?ying altitude (H)	100 m
Number of slots (T)	80
RSU altitude (h_0)	5 m
Bandwidth of VUE channel (W)	10 MHz
UAV Maximum Flight Distance (V_{max})	2.5m
Pathloss exponent (θ)	4
Log-normal shadowing standard deviation	10 dB

IV. Simulation Results and Performance Analysis

In this subsection, in order to test the effectiveness of the algorithms and to evaluate their performance, we provide numerical simulation results that mainly evaluate the performance of the joint optimisation of the UAV trajectory and the channel power allocation scheme, and present two schemes, the UAV hovering over a fixed position scheme and the way of fixing the UAV trajectory, and compare our scheme with them. In the hovering scheme, the UAV hovers above the fixed position to simplify the computational complexity, in which we simulate a two-way lane with a length of 800 m and a width of 30 m. Unless otherwise specified, six vehicles are selected for the simulation on the road, in which each vehicle travels in a straight line at a constant speed with different speeds. The main parameters in the simulation are shown in Table II.

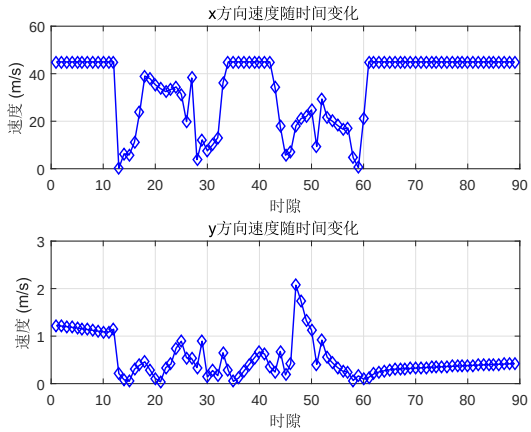

Fig. 3: UAVspeed

Firstly, we show the optimisation of the UAV trajectory when the total energy efficiency of the system is maximised for different time slots as shown in Fig. 2, where the black arrow represents the vehicle travelling to the right as the positive direction, and we stipulate that the UAV flies from a fixed

starting point to a fixed end point. We find that when the task time is sufficient, the UAV will tend to stick close to the vehicle that is far away from the base station to serve it.Figure 3 shows the speed of the drone at each time slot, when the vehicle needs drone assistance, the drone will slow down or even hover to match the vehicle speed for it.

After verifying the performance of the optimised trajectory of the algorithm, the performance level of the proposed scheme under different parameters is further verified. Fig. 4 shows that when using the different θ, they have different effects on the energy efficiency of the system at different time slots when using different θ. The θ is a coefficient that describes the relative energy cost of the vehicle task at the drone end versus the roadside unit end. When θ changes, the system utility also changes. Higher parameters represent a greater focus on the UAV's flight energy consumption. The overall system energy efficiency decreases as the UAV flight time T increases, as longer time is sufficient for the UAV to traverse more vehicles to obtain better channels and save energy. In addition, we find that a lower θ leads to higher energy efficiency. This is because when we consider the UAV's energy consumption to be relatively important, vehicles tend to increase their power to transmit more data, thus increasing energy efficiency.

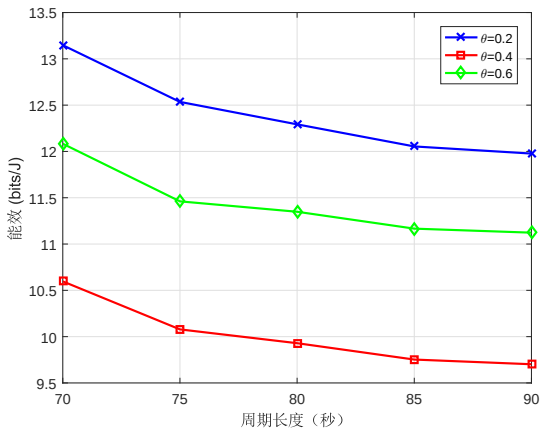

Fig. 4: diffthetθ

In Fig. 5, we compare the energy efficiency performance of the three UAV communication schemes, OPTS, FPHS and FTS, under different flight cycles T . From the overall trend, the energy efficiency of each scheme gradually stabilises as the UAV's flight time increases, which is due to the fact that the UAV has more sufficient time to transmit data at the right power. Further observation reveals that the two schemes, OPTS and FPHS, are suitable for different scenarios. Despite the higher complexity of the OPTS algorithm, it is able to achieve higher energy efficiency in a shorter flight cycle, showing better timeliness. This means that OPTS is an advantageous choice in situations where fast response is required. Comparatively, when the flight cycle is longer, the energy efficiency of FPHS, although slightly inferior to OPTS, is simpler to implement due to its lower algorithmic complexity. Therefore, in environments with less stringent time requirements, FPHS may be a more economical solution. As for the FPHS solution, its energy efficiency performance is relatively poor. This is due to the fact that the UAV hovers at a fixed position, resulting in a long distance from the ground vehicle, which affects the efficiency of data transmission. In addition, as the flight cycle increases, the energy efficiency gap between OPTS and FPHS gradually narrows. This is mainly due to the fact that when the flight cycle is short, the data transmission time in the OPTS is limited and the vehicle needs to send information to the UAV within a limited time, which leads to a decrease in energy efficiency. Whereas, as the flight cycle increases, the OPTS has more time to optimise the data transmission process, which leads to improved energy efficiency.

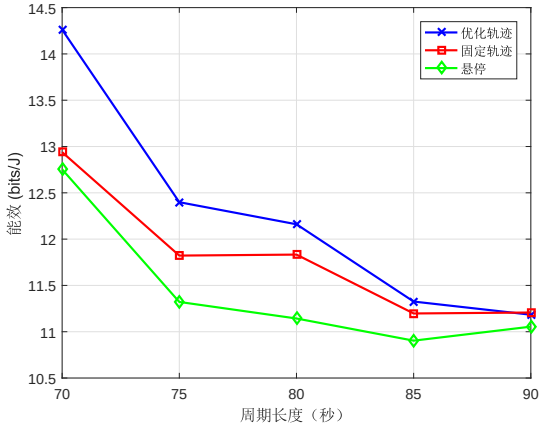

Fig. 5: DifferentSchemes

The following figure shows the comparison of the three schemes with different parameters θ.

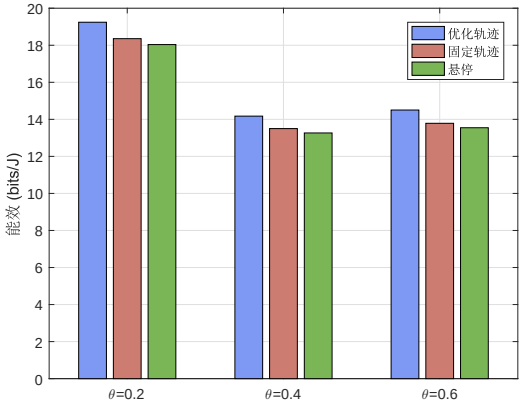

Fig. 6: DifferentSchemesANDdiffthetθ

In Fig. 6, we explore how the energy efficiency of three UAV communication scenarios, OPTS, FHCS and FTS, varies with the parameter θ. The θ is a key parameter that reflects the weighting of the relative energy cost between the UAV's flight energy consumption and its communication energy consumption. When the value of θ is large, the UAV's flight energy consumption becomes the dominant factor in the overall energy consumption. Observing the trend in the figure, we

can find that with the change of θ, the energy efficiency of all the three scenarios undergoes a significant decreasing process and reaches the lowest point at $\theta = 0.8$. Subsequently, the energy efficiency shows a slightly increasing trend. When θ is small, it means that the UAV's flight energy consumption accounts for a relatively low percentage of the overall energy cost. As a result, the UAV can transmit data more aggressively, which improves the overall energy efficiency. On the contrary, when θ is large, the UAV's flight energy consumption becomes dominant, which restricts its ability to transmit data, and thus affects energy efficiency. In summary, the parameter θ affects the energy efficiency performance of the three UAV communication schemes by influencing the energy cost distribution between the UAV's flight energy consumption and communication energy consumption. In practical applications, we need to choose the appropriate θ value according to specific scenarios and requirements in order to optimise the communication efficiency of UAVs.

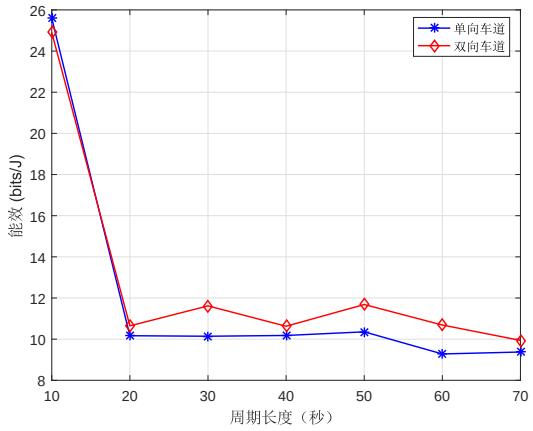

Fig. 7: twoway

Finally Fig. 7 compares the two-way lane scenario with the one-way lane scenario, which brings higher energy efficiency due to the fact that the two-way lane scenario can utilize the synergy between the roadside unit and the airborne base station to a greater extent, given that the total number of vehicles on the road is the same.

V. Conclusions

In this paper, we propose an efficient air-ground integrated UAV-assisted vehicular communication scheme for two-way lanes. In this paper, we propose a basic balancing scheme between the throughput during vehicular communication and the energy consumption for communication and UAV flight. By optimising the vehicle's transmit power and the UAV's flight trajectory, as well as the allocation of time slots, the energy efficiency of the system can be maximised, and the quality of service of vehicular communication is guaranteed by probabilistic constraints, which can be found to affect the energy efficiency of the system by adjusting different parameters θ. By comparing different UAV flight scenarios, it can be seen that the UAV scenario with optimised trajectory is the best. At the same time, this chapter also studies the more realistic scenario of directional lanes roadside units and servers are often deployed on one side of the road, so in the two-way lane scenario, there is always always a vehicle will be driving away from the roadside unit, thus causing communication difficulties, we use the drone to assist its communication can be a better solution to the difficulty.

References

[1] F. Liu, Z. Chen, and B. Xia, "Data dissemination with network coding in Two-Way Vehicle-to-Vehicle networks," *IEEE Transactions on Vehicular Technology*, vol. 65, no. 4, pp. 2445–2456, 2016.

[2] Z. Zhang, G. Mao, and B. D. O. Anderson, "On the information propagation process in mobile vehicular ad hoc networks," *IEEE Transactions on Vehicular Technology*, vol. 60, no. 5, pp. 2314–2325, 2011.

[3] E. Baccelli, P. Jacquet, B. Mans, and G. Rodolakis, "Highway vehicular delay tolerant networks: Information propagation speed properties," *IEEE Transactions on Information Theory*, vol. 58, no. 3, pp. 1743–1756, 2012.

[4] Z. Zhang, G. Mao, and B. D. O. Anderson, "Stochastic characterization of information propagation process in vehicular ad hoc networks," *IEEE Transactions on Intelligent Transportation Systems*, vol. 15, no. 1, pp. 122–135, 2014.

[5] H. Wu, R. M. Fujimoto, G. F. Riley, and M. Hunter, "Spatial propagation of information in vehicular networks," *IEEE Transactions on Vehicular Technology*, vol. 58, no. 1, pp. 420–431, 2009.

[6] M. Fiore and J. Härri, "The networking shape of vehicular mobility." New York, NY, USA: Association for Computing Machinery, 2008.

[7] Y. Liang, L. Xiao, D. Yang, Y. Liu, and T. Zhang, "Joint trajectory and resource optimization for UAV-Aided Two-Way relay networks," *IEEE Transactions on Vehicular Technology*, vol. 71, no. 1, pp. 639–652, 2022.